Catalytic Decomposition of N_2O: Best Achievable Methods and Processes

Paschalia Taniou [a] **, Zoe Ziaka** [a*] **, Savvas Vasileiadis** [a]

[a] *Department of Science and Technology, Laboratory of Environmental Catalysis, Hellenic Open University, Patras, GREECE.*

ARTICLE INFO	ABSTRACT
	In the current review paper, the N_2O direct decomposition was investigated over a series of different catalytic systems, containing metals, zeolites, cobalt spinels. The N_2O split via catalysis and the use of membrane systems in the separation to molecules N_2 and O_2 were studied, too. Decomposition of N_2O has been studied in the temperature rate of 673 to 873 K over supported catalysts of chemical elements: Pd, Rh, Ru, Ni, Pt, Zn, Fe, Cu, Ir, over γ-Al_2O_3 showing their best catalytic activity. M-zeolites, (M = Cu, Fe, Co, etc.) supported on perovskite or precious metals such as Pd, Rh zeolites and dominant iron and copper catalytic structures such as ZSM-5, MFI, BEA, BETA investigated in the temperature rate of 583 to 775 K with best catalytic activity. Iron zeolites are more prevalent at high concentrations showing good catalytic behavior only at high temperatures. The spinel catalyst $Zn_{0.36}Co_{0.64}Co_2O_4$ and Rh/Mullite catalyst offer up to complete N_2O conversion.

1. Introduction

It is well known that nitrous oxide is considered a dangerous environmental pollutant because it contributes to the destruction of stratospheric ozone and simultaneously is also considered as a
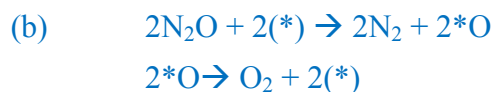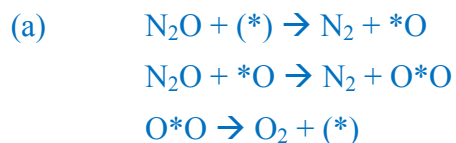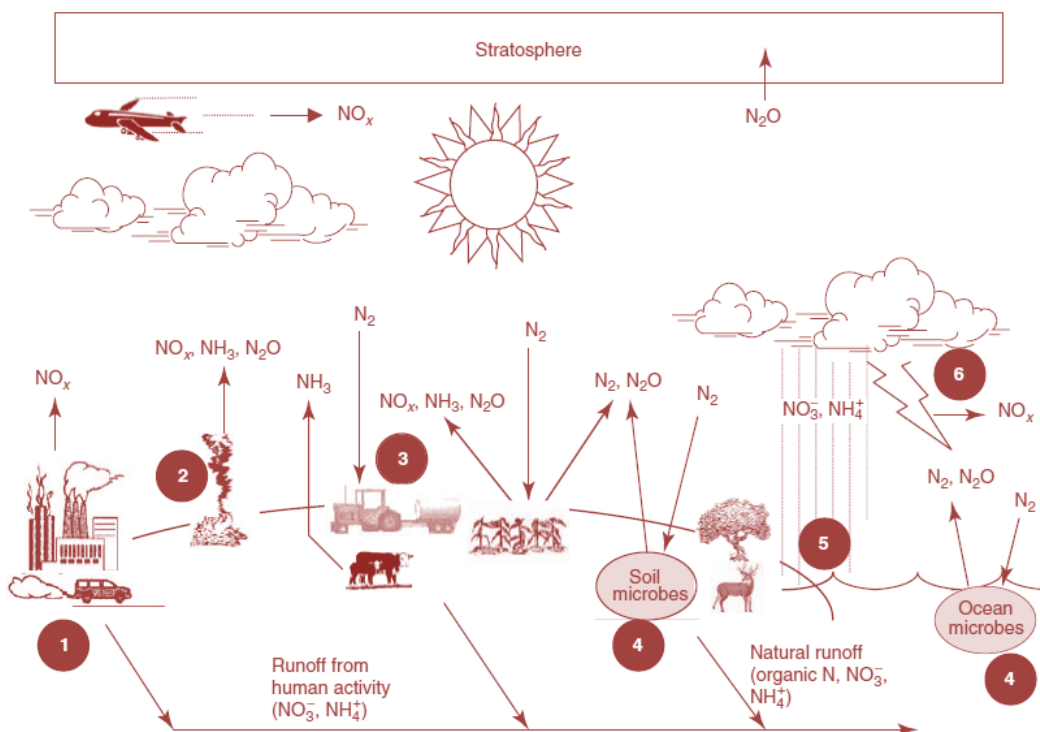
greenhouse gas. The concentration of N_2O in the atmosphere increases every year up to 0.2–0.3%, and this increase is caused mainly by anthropogenic activities. More specific, chemical processes related to the production and use of nitric acid and fluidized bed combustion are the two main nitrous oxide sources, and their contribution to the total nitrous oxide emissions amounts up to 20%. Minimization of N_2O emission can be accomplished mainly by two ways, either by lowering the formation of N_2O or after treatment where catalysis introduces the N_2O abatement by the direct decomposition into nitrogen and oxygen. Metal such as transition metal oxides, zeolites and noble metals, especially rhodium, dispersed on oxide supports exhibit catalytic activity in N_2O decomposition. [1]

Nitrous oxide (N_2O), for many years has not received the attention of scientific interest. But, in recent years, due to the significant impact of greenhouse gases in the atmosphere and the increasing annual concentration a research activity has started, which involves various processes and technologies of reduction of it and splitting into harmless molecules, N_2 and O_2.

A well understandable picture of the global nitrogen cycle is shown in Figure 1. (1) urban areas: NO_x is produced from high-temperature combustion. (2) Biomass burning: NO_x, NH_3, and N_2O are produced from combustion of plant materials. (3) Agriculture: nitrogen is fixed through fertilizer manufacturing and the planting of nitrogen-fixing crops. Denitrification produces N_2 and N_2O. NH_3 is produced from fertilizer use and livestock excreta. (4) Natural fluxes: nitrogen fixing microbes in soil and sea water supply plants with usable nitrogen. Denitrification releases N_2 and N_2O to atmosphere. (5) Wet and dry deposition: Nitrate and ammonia are removed from the atmosphere to both land and sea. (6) Lightning: NO_x is produced via high-temperature reaction of N_2 and O_2. [2]

The following mechanisms is proposed for the direct N_2O decomposition:

(a) $N_2O + (*) \rightarrow N_2 + *O$
       $N_2O + *O \rightarrow N_2 + O*O$
       $O*O \rightarrow O_2 + (*)$

(b) $2N_2O + 2(*) \rightarrow 2N_2 + 2*O$
       $2*O \rightarrow O_2 + 2(*)$

(c) $N_2O + (*) \rightarrow N_2 + *O$

Paschalia Taniou, Zoe Ziaka, and Savvas Vasileiadis

$$N_2O + *O \rightarrow N_2 + *O_2$$
$$N_2O + *O_2 \rightarrow N_2 + *O_3$$
$$*O3 \rightarrow *O + O_2$$

Figure 1: Nitrogen cycle [2].

In mechanism (b) (Langmuir–Hinshelwood mechanism), the migration of oxygen from one active site (*) followed by recombination with another oxidized site is the rate-determining step. This reaction mechanism requires the active participation of, at least, two iron centers that are not necessarily located in adjacent positions. In mechanisms (a) and (c) (Eley–Rideal mechanisms), N_2O decomposition and oxygen evolution occur at the same isolated sites (*) after successive collisions between N_2O with (*) and *O for (a), and with (*), *O, and $*O_2$ for (c). The proposed above mechanisms are all in agreement with transient response experiments, showing that N_2 appears before O_2 upon direct N_2O decomposition pulses in the 773 to 848 K temperature range. This is happens because in all cases the global decomposition reaction is limited by the reactions steps leading to gas O_2. More specific, recently accurate temporal analysis of products strongly implies that mechanism (a) is the most likely. On the other hand, from the point of view of the oxygen species formed on iron active sites (*), the three mechanisms are associated with increasingly complex oxygen species: *O, O*O, and $*O_2$ for (a); *O for (b); and *O, $*O_2$ and

* Corresponding author (Z. Ziaka). Tel/Fax: +30-2310-275473 E-mail addresses:
bookeng@hotmail.com, z.ziaka@ihu.edu.gr.

*O_3 for (c). [3]

The anthropogenic sources of N_2O emissions from the Annex I group are differentiated, as shown in Table 1, which is based on UNFCCC data (UNFCCC, 2009b). The energy and industrial processes of N_2O emission sources contributed to ca.12% and 10% of total N_2O emissions in the year 2007, respectively. If we compare the net emissions between the years 1990 and 2007, the N_2O emissions generated by agriculture are decreased significantly over that period, but yet the extent of reduction was much higher in industrial processes than in the agricultural sector. As an explanation, one can say that it is possible to accomplish such a high degree of reduction in the volume of emissions generated by industrial processes because the N_2O produced by those sources is likely destructed by using conventional N_2O decomposition technologies. [4]

Table 1: Net emissions of N_2O from the anthropogenic sources by members of the Annex I group (UNFCCC, 2009b)

Sources	1990 Net emission[a]	2007 Net emission[a]	Difference of emission[b]	Reduction [c] %
Energy	119,665	113,535	6130	5
Industrial processes	184,387	91,983	92,404	50
Solvent and other product use	10,994	9,863	1081	10
agriculture	895,550	695,811	199,739	22
LULUCI[d]	10,825	14,367	-3542	-33
Waste	28,005	31,120	-3115	-11
other	32	33	-1	-3
Total	1,249,408	956,712	292,696	23

[a] Annual emission in terms of 1000 tons CO_2 equivalent.
[b] Net emission in 1990- net emission in 2007.
[c] (Net emission in 1990- net emission in 2007)/ net emission in 1990 x 100.
[d] Land use, land-use change and forestry.

Moreover, the number of clean development mechanism (CDM) projects aimed at reducing N_2O emissions has increased the last years. Although N_2O reduction projects account for only 2.6% of all CDM projects, these N_2O reduction projects account for 13% of the total reduction of all greenhouse gases measured on a CO_2 equivalent basis regarding the CDM. Specifically, China is the host nation for half of all N_2O CDM reduction projects while approximately 78% of the N_2O reduction technologies for these CDM projects come from Japan, the UK, and Switzerland. N_2O reduction in CDM projects has been applied to production plants for such chemicals as nitric acid, adipic acid, and caprolactam. The relevant technologies for N_2O reduction used in CDM projects are thermal or catalytic decomposition and selective catalytic reduction with the selection of an

Paschalia Taniou, Zoe Ziaka, and Savvas Vasileiadis

appropriate reduction strategy dependent on the specifications of the production process.

Thirty-nine case studies for the N_2O decomposition have been investigated and examined [45], and in this paper among them we present the best catalytic application of the N_2O decomposition through the catalytic systems below including [37], [38] [39], [40]:

- Split N_2O on Supported Catalysts
- Split N_2O on Zeolite catalysts
- Split N_2O over cobalt Spinels
- Split N_2O over rhodium catalyst
- Split N_2O over Cu Catalysts

In addition, it has been also studied the case of N_2O separation into nitrogen and oxygen via photocatalysis ([41], [42]) and via membranes (six case studies), [34].

Moreover, nitrogen gas, N_2, is the most abundant gas in the atmosphere at 78.1% by volume. In terms of physical properties, Nitrogen is a colorless gas at room temperature. Although N_2 is generally quite inert chemically, it is utilized by nitrogen-fixing organisms and this is the primary natural nitrogen input to terrestrial and marine ecosystems. However, biological nitrogen fixation refers to the natural process that is performed by a variety of bacteria and algae, both symbiotic and free living. On the other side, industrial nitrogen fixation refers to the industrial production of NH_3 and nitrates from N_2, mainly for fertilizers. In addition, nitrogen-fixing organisms are resided on the roots of many leguminous plants (clover, soybeans, chickpeas, etc.) and have been utilized agriculturally as a mean of replenishing soil nitrogen ("green manures").

The natural flux of N_2 from the atmosphere to oceans and terrestrial ecosystems is balanced by an almost equal source of N_2 to the atmosphere in a process called denitrification. In denitrification, certain microbes utilize aqueous NO_3^- ion as an oxidant in low-oxygen environments. Thus, the combined effects of natural biological nitrogen fixation and denitrification result in a nearly balanced cycle with respect to the atmospheric N_2. Denitrification releases a smaller amount of N_2O, as well.

As mentioned earlier, Nitrous oxide, or N_2O, is a colorless, fairly unreactive gas at room

temperature. It is also the second most abundant nitrogen compound in the atmosphere with a current (year 2000) average global mixing ratio of 316 parts per billion by volume (ppbv). Because of its low reactivity and low water solubility, N_2O has a lifetime of about 100 years in the atmosphere and is well mixed throughout the global troposphere. Due the fact that it has no significant sinks in the troposphere, N_2O eventually gets transported to the stratosphere where it can react or photolyze. The products of this decomposition demonstrate an important parameter in the chemistry of the stratosphere. In denitrification, 80 to 100% of the nitrogen released is in the form of N_2, with the remainder being N_2O, although under certain environmental conditions, nitrous oxide can end up as a major end product.

Although denitrification is a natural process, there is an important increase in denitrification and N_2O release coming from the application of nitrogenous fertilizers, which is indeed a certain contributor to the global increase in observed N_2O concentrations. Moreover, N_2O is produced as well from biomass burning.

Because of these additional anthropogenic contributions, N_2O sources are now higher than the sinks and N_2O is accumulating in the atmosphere. Because N_2O is a greenhouse gas and shows an important impact in the stratospheric ozone depletion, considering the contributions from agricultural releases and biomass burning of N_2O and, if possible, minimizing these fluxes are new areas of further investigation.

Table 2 shows the global average lifetime, global average mixing ratio or the range of observed mixing ratios, and an estimate of the global burden for some of the key nitrogen species. Long-lived compounds, such as N_2 and N_2O, have very uniform distributions throughout the globe. This helps us to determine easily their total abundance and average global concentration based on a relatively small number of observations. However, short-lived species, such as NO_x and NH_3, have highly inhomogeneous distributions, which make it much more difficult to determine their global abundance. For example, the NO_x mixing ratios vary over 5 orders of magnitude between urban and remote regions.

Furthermore, for both NO_x and NH_3, the lifetime is dependent on local conditions. For NO_x, the lifetime in urban air due to reaction with OH is about half a day, whereas in the upper troposphere it can be many days, depending on the OH molecular density. So for both NO_x and

Paschalia Taniou, Zoe Ziaka, and Savvas Vasileiadis

NH_3, the global burdens have high uncertainties, on the order of $\pm100\%$. For N_2O, there is good evidence that modern-day mixing ratios are larger than pre-industrial values by 12–15%. This outcome is based on direct atmospheric observations over the past two decades and ice core data extending back several thousand years.

Figure 2 shows recent atmospheric data, collected at four background stations by the National Oceanographic and Atmospheric Administration's Climate Monitoring and Diagnostics Laboratory (NOAA–CMDL). Besides, it is shown an estimate of the pre-industrial mixing ratio of N_2O, as determined by ice core data. For NH_3 and NO_x, the global burden has certainly increased significantly as a result of human contribution; however, due to the highly variable nature of these reactive gases, it is difficult to quantify the exact amounts. [2]

Table 2: Mixing ratios and burdens of atmospheric nitrogen compounds. The N_2O mixing ratio is rising by 0.7 ppbv per year. These values are for the year 2000.

compound	lifetime	global mean value	global burden (tgN)
N_2	Millions of years	78.08%	3.9×10^9
N_2O	~100 years	316 ppbv	1600
NH_3	~3 years	0.05-50 ppbv	~0.4
NO_X	~1 day	0.005-200 ppbv	~0.2
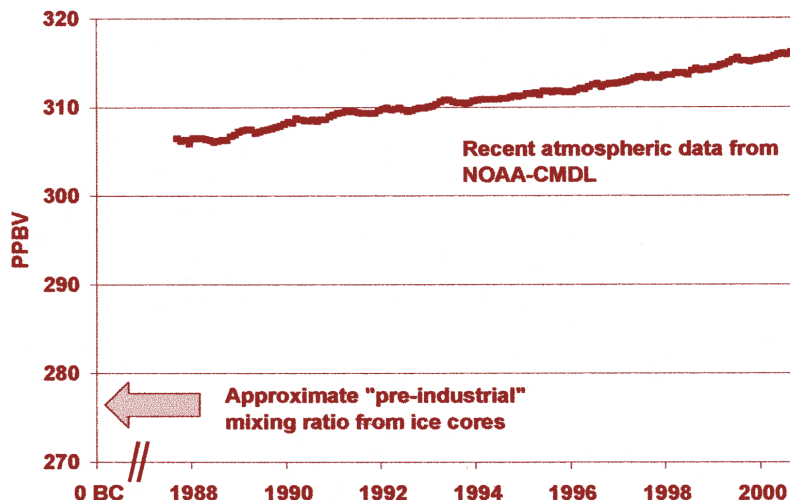
Figure2: Global average N_2O mixing ratio (ppbv) from recent atmospheric data and estimated from ice core data. The NOAA-CMDL data are based on observations made at four background stations [2].

After the Kyoto Protocol regulation for the emission of six green- house gases (CO_2, CH_4,

N_2O, HFCs, PFCs and SF_6), a number of clean development mechanism (CDM) projects has been registered under the United Nations Framework Convention on Climate Change (UNFCCC). CDM projects have been developed to assist the reduction of greenhouse gas emissions in developing countries included in the non-Annex I group, by allowing them to earn certified emission reduction (CER) credits which can be traded and used by industrialized countries in the Annex I group. Since the CDM targets the reduction of greenhouse gas (GHG) emissions in developing countries, an acceleration of technology transfer has been introduced from developed countries to the developing ones. Moreover, CDM projects stimulate the development of reduction technology to obtain more CER credits. Furthermore, emissions by greenhouse gas sources have been reported in order to systemize them for CDM projects.

Table 3: Net emissions of each greenhouse gases by members of the Annex I group (UNFCCC, 2009b)

Gas	Net emission [a] 1990	Net emission [a] 2007	Difference of emission [b]	Reduction [c] %
CO_2	13,514,353	13,375,386	138,967	1
CH_4	2,248,913	1,906,667	342,246	15.2
N_2O	1,249,408	956,712	292,696	23.4
Aggregated F-gases[d]	267,111	308,379	-41,267	-5.4
Total	17,279,785	16,547,143	732,642	42

[a] Annual emission in terms of 1000 tons CO_2 equivalent.
[b] Net emission in 1990- net emission in 2007.
[c] (Net emission in 1990- net emission in 2007)/ net emission in 1990 x 100.
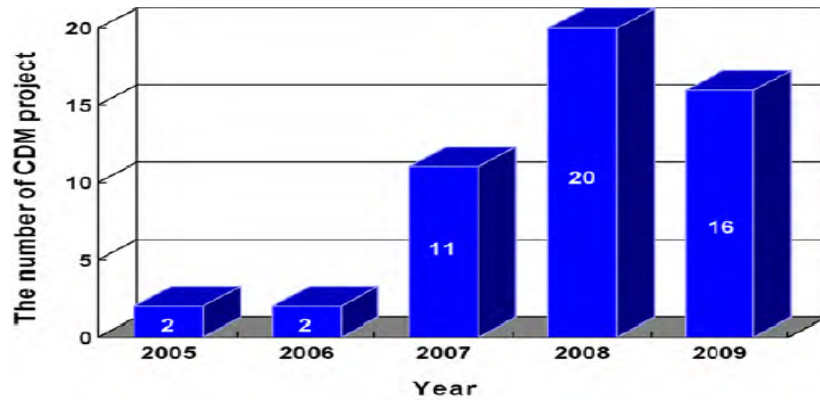[d] HFCs, PFCs, SF_6

Tables 1 and 3, show the net emission of each greenhouse gas by members of the Annex I group from the years 1990 to 2007 for comparison, based on data provided by the UNFCCC (UNFCCC, 2009a). Although CO_2 accounts for ca.81% of all net greenhouse gas emissions in 2007, the reduction of CO_2 is low in comparison with that of CH_4 and N_2O. On the other hand, it has been presented that the reduction of N_2O is quite high compared with other greenhouse gases, even though the amount by which N_2O emissions has been reduced is at a lower degree than that of the CH_4. For this reason, the reduction of N_2O rather than other greenhouse gases is bound to attract more interest in CDM projects. The anthropogenic sources of N_2O emissions from the Annex I group are varied, as shown in Tables 1 and 3, which is based on UNFCCC data (UNFCCC, 2009b). The energy and industrial processes of N_2O emission sources contributed to ca.12% and 10% of total N_2O emissions in the year 2007, respectively. If we compare net emissions between the years 1990 and 2007, N_2O emissions generated by agriculture decreased considerably over that period, yet the extent of reduction is much higher in industrial processes than in the agricultural sector. It

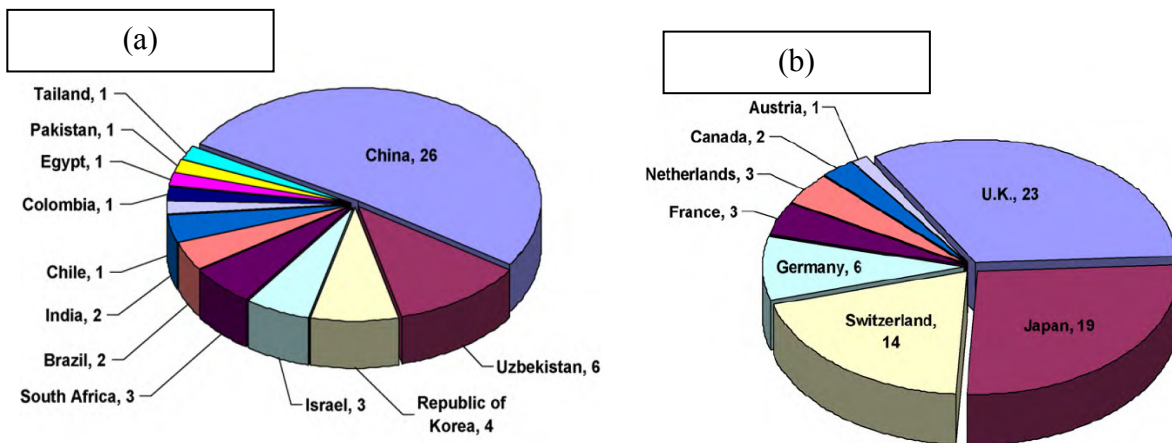Paschalia Taniou, Zoe Ziaka, and Savvas Vasileiadis

was possible to accomplish such a high degree of reduction in the volume of emissions generated by industrial processes because, as it was addressed before, the N_2O produced by those processes is likely destructed by using conventional N_2O decomposition technologies. Thus, the Annex I group has tried to transfer the technologies to the non-Annex I group via the implementation of CDM projects. This paper investigates the present status and trends of CDM projects for N_2O reduction, and proposes a possible future direction for CDM projects.

## Present status of CDM projects to reduce N_2O emissions

By December 2009, a total of 1952 CDM projects had been registered with the UNFCCC, from which 2.6% were related to N_2O reduction, showing a sharp increase in the number of CDM projects aimed at N_2O reduction since 2007 (see Figure 3) (UNFCCC, 2009c). Despite the small number of CDM projects contributing to the reduction of the N_2O emissions, it is worthy to be addressed that the reduction of N_2O emissions in terms of their CO_2 equivalence accounts for 13% of the total reduction of all greenhouse gases. There are 12 countries that host CDM projects for N_2O reduction, namely China, Uzbekistan, Republic of Korea, Israel, South Africa, Brazil, India, Chile, Colombia, Egypt, Pakistan and Thailand. China and Uzbekistan have registered 50% and 11.5% of the total number of the CDM projects, respectively (see Figure 4a) (UNFCCC, 2009c). For the CDM projects involving the reduction of N_2O, eight nations –the U.K., Japan, Switzerland, Germany, France, the Netherlands, Canada and Austria have considered the host parties with new technologies for N_2O reduction. The U.K., Japan and Switzerland have contributed 32.4%, 26.7% and 19.7% of the technology transfer, respectively (see Figure 4b) (UNFCCC, 2009c). The transferred technologies were employed to reduce N_2O emitted by industrial processes involved in the production of chemicals such as nitric acid, adipic acid and caprolactam. With respect to the CDM projects, the applied industrial process consists of 90% nitric acid, 7.8% adipic acid and 1.9% caprolactam, as shown in Figure 5 (UNFCCC, 2009c). The large number of projects target in nitric acid production may be contributed to the application of various technologies to N_2O reduction. The technical measures for baseline and monitoring in the CDM projects are described in methodologies of the CDM projects. [4]

* Corresponding author (Z. Ziaka). Tel/Fax: +30-2310-275473 E-mail addresses: bookeng@hotmail.com, z.ziaka@ihu.edu.gr.

Figure 3: The annual number of CDM projects for N_2O reduction (UNFCCC, 2009c) [4]
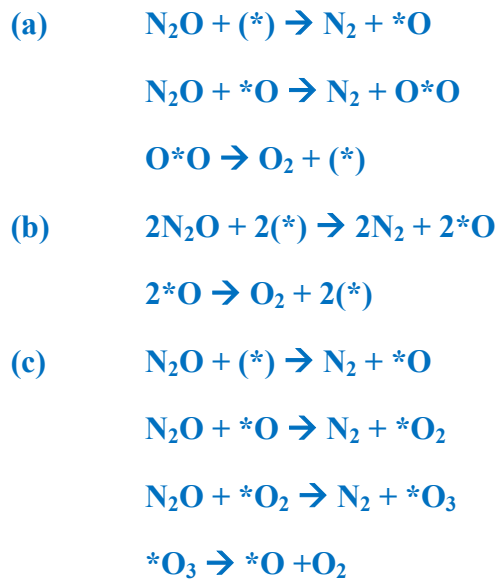

Figure 4: The number of CDM projects for N_2O reduction a) the host parties, b) the technology suppliers   (UNFCCC, 2009c) [4].
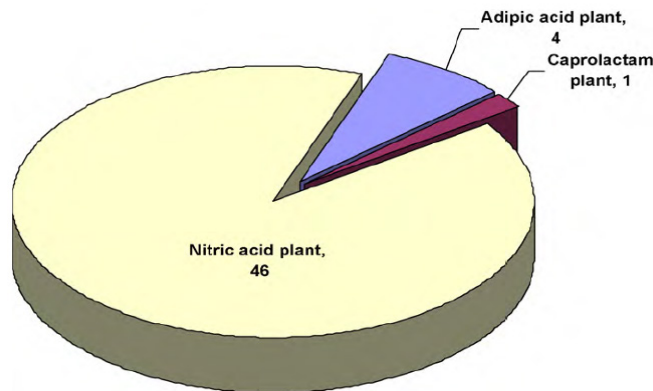
Figure 5: The number of CDM projects for N_2O reduction in industrial processes   (UNFCCC, 2009c) [4].

The proposed mechanism in direct N_2O decomposition

The most popular mechanisms in direct N_2O decomposition are presented as follows:

Paschalia Taniou, Zoe Ziaka, and Savvas Vasileiadis

(a) $N_2O + (*) \rightarrow N_2 + *O$

$N_2O + *O \rightarrow N_2 + O*O$

$O*O \rightarrow O_2 + (*)$

(b) $2N_2O + 2(*) \rightarrow 2N_2 + 2*O$

$2*O \rightarrow O_2 + 2(*)$

(c) $N_2O + (*) \rightarrow N_2 + *O$

$N_2O + *O \rightarrow N_2 + *O_2$

$N_2O + *O_2 \rightarrow N_2 + *O_3$

$*O_3 \rightarrow *O + O_2$

In mechanism (b) (Langmuir–Hinshelwood mechanism), the migration of oxygen from one active site (*) followed by recombination with another oxidized site is the rate-determining step. This proposed reaction mechanism implies the active participation of at least two iron centers that are not necessarily located in adjacent positions. In mechanisms (a) and (c) (Eley–Rideal mechanisms), N_2O decomposition and oxygen evolution happen at the same isolated sites (*) after successive collisions between N_2O with (*) and *O for (a), and with (*), *O, and $*O_2$ for (c). The above analyzed mechanisms are all in a good agreement with transient response experiments, indicating that N_2 appears before O_2 upon direct N_2O decomposition pulses in the 773 to 848 K temperature range. This happens because in all cases the global decomposition reaction is limited by the reaction steps leading to O_2 gas phase.

More recent accurate temporal analysis of products strongly implies that mechanism (a) is the most likely. On the other hand, from the point of view of the oxygen species formed on iron active sites (*), the three mechanisms are associated with increasingly complex oxygen species: *O and O*O for (a); *O for (b); and *O, $*O_2$, and $*O_3$ for (c).

2. Study Details and Discussion

Best case study 1: N_2O Abatement Over γ-Al_2O_3 Supported Catalysts.

Numerous catalytic systems, such as supported or unsupported noble metals, pure oxides,

mixed oxides, are reported to be active for N_2O decomposition/ reduction reactions [5], [6], [7].

Catalyst.

Through their study in 2009, G. Pekridis et al. [7], investigated the effect of excess oxygen and reducing agents (CH_4 and C_3H_8) on N_2O decomposition, over a series of noble and transition metal catalysts (Pd, Rh, Ru, Cu, Fe, In and Ni), supported on γ-Al_2O_3 carrier. It was noticed that N_2O decomposition rate was inhibited by oxygen, whereas the catalytic activity was generally increased in the presence of reducing agents, with C_3H_8 to be more efficient than CH_4. [7]

Materials and Reaction System.

A series of Pd-, Rh-, Ru-, Cu-, Fe-, In-, and Ni-based on alumina catalysts were prepared using the dry impregnation method. Water solutions of the corresponding metal salts were impregnated on γ-Al_2O_3 carrier (Engelhard, 180–355 μm) so as to yield 2.0 wt% metal loading.

After impregnation took place, the catalysts were dried at 120 ^oC for 2 h and then were calcined at 600 ^oC for 4 h under air flow. The actual metal content was measured using ICP-AES, while the BET surface areas of the samples were measured at 77 K with an Autosorb-1 apparatus.

All the catalysts prepared in the present work are listed in Table 4 along with the corresponding precursor materials used, their actual metal loading, and BET surface areas.

Table 4: List of prepared catalysts.

Type of Catalyst	Precursor		Metal loading (%w/w)		Surface area (m^2/g)
			Nominal	ICP measured	
γ-Al_2O_3	-	-	-	-	209
Pd/γ-Al_2O_3	$Pd(NO_3)_2.2H_2O$		2	2.078 ± 0.075	173
Rh/γ-Al_2O_3	$RhCl_3.3H_2O$		2	1.917 ± 0.045	170
Ru/γ-Al_2O_3	$RuCl.H_2O$		2	Not measured	192
Cu/γ-Al_2O_3	$Cu(NO_3)_2 .3H_2O$		2	1.992 ± 0.060	175
Fe/γ-Al_2O_3	$Fe(NO_3)_3.9H_2O$		2	1.960 ± 0.050	171
In/γ-Al_2O_3	$In(NO_3)_3.5H_2O$		2	2.090 ± 0.070	184
Ni/γ-Al_2O_3	$Ni(NO_3)_2.6H_2O$		2	1.925 ± 0.050	129

Paschalia Taniou, Zoe Ziaka, and Savvas Vasileiadis
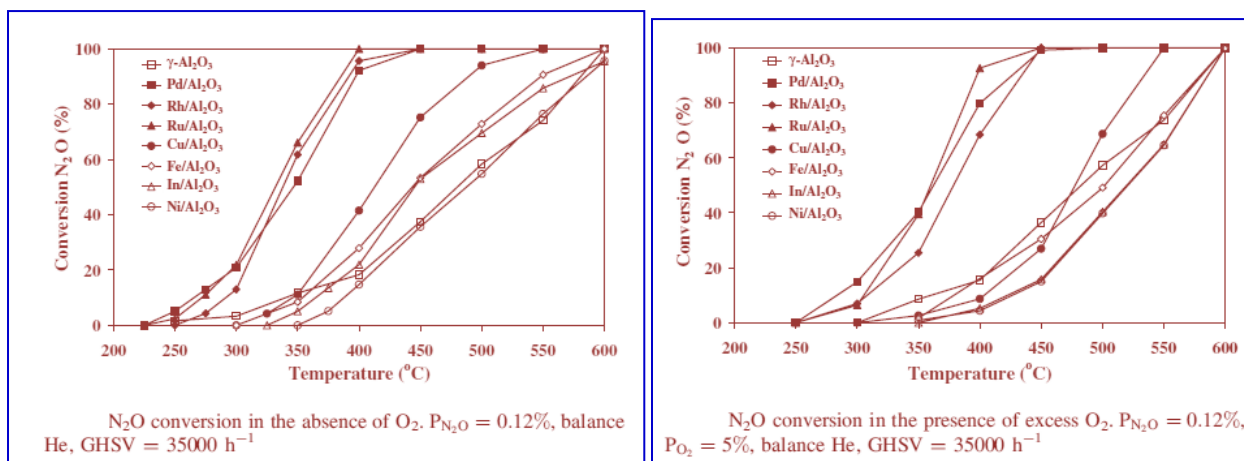
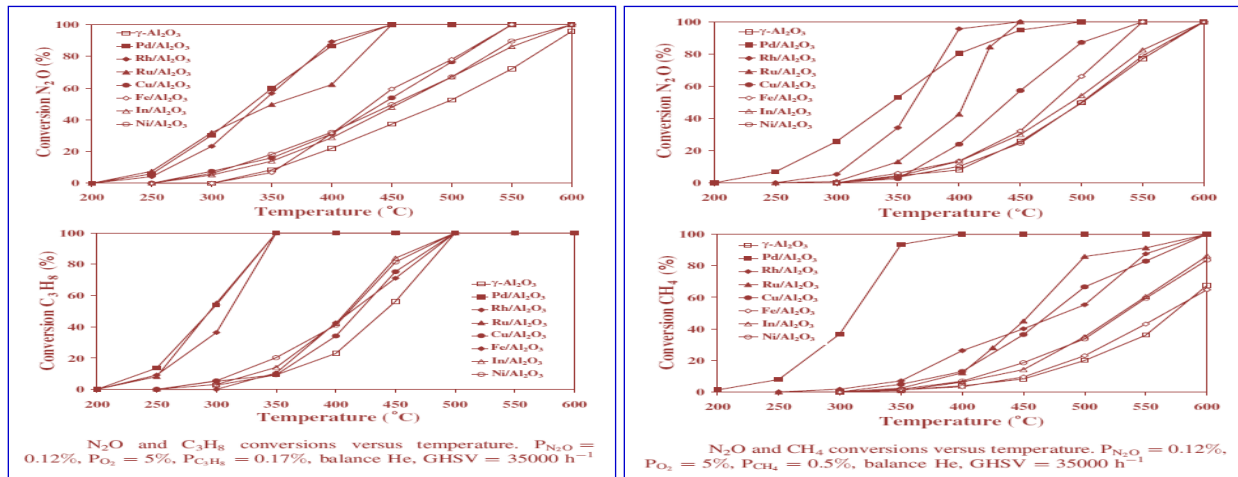**Figure 6:** Effect of Catalyst Entity and Gas Phase Oxygen on the N_2O Decomposition [7].

Analysis.

Analyzing the experimental observations, the current results show that N_2O decomposition is the major pathway for N_2O abatement even in the presence of hydrocarbons; it works mainly as oxygen scavengers reducing the metal active sites. The different observed efficiencies of C_3H_8 and CH_4 can be explained by taking into account their different interaction with the catalyst's surface and consequently their capability to take away surface oxygen ad-atoms originated either from N_2O decomposition and/or gas phase oxygen dissociative adsorption.
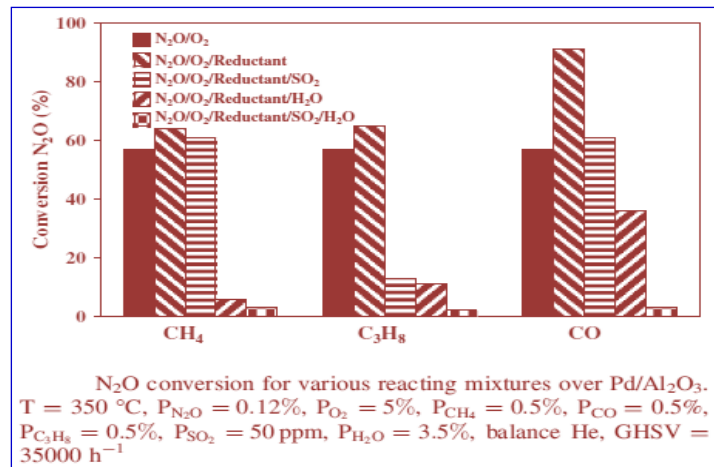
Pure γ-alumina and alumina-supported catalysts were initially tested for the N_2O decomposition to N_2 (the only N-containing product) in the absence of oxygen at the temperature range of $200 – 600^oC$.

Following, all catalysts were inhibited by the presence of oxygen in the gas phase, as oxygen is dissociatively adsorbed on the catalyst's surface to yield strongly chemisorbed oxygen species, identical to those produced by the N_2O decomposition. As a result a monoatomic oxygen layer is formed, hindering the reaction. The effect of catalyst entity and gas phase oxygen on the N_2O decomposition is shown in the Figure 6:

* Corresponding author (Z. Ziaka). Tel/Fax: +30-2310-275473 E-mail addresses: bookeng@hotmail.com, z.ziaka@ihu.edu.gr.

The effect of reducing agent on the N_2O reduction at lean conditions is shown in a combined set in Figure 7 [7].

N₂O and C₃H₈ conversions versus temperature. P_{N_2O} = 0.12%, P_{O_2} = 5%, $P_{C_3H_8}$ = 0.17%, balance He, GHSV = 35000 h^{-1}

N₂O and CH₄ conversions versus temperature. P_{N_2O} = 0.12%, P_{O_2} = 5%, P_{CH_4} = 0.5%, balance He, GHSV = 35000 h^{-1}

Figure 7: The effect of reducing agent on the N_2O reduction at Lean Conditions [7].

N₂O conversion for various reacting mixtures over Pd/Al_2O_3. T = 350 °C, P_{N_2O} = 0.12%, P_{O_2} = 5%, P_{CH_4} = 0.5%, P_{CO} = 0.5%, $P_{C_3H_8}$ = 0.5%, P_{SO_2} = 50 ppm, P_{H_2O} = 3.5%, balance He, GHSV = 35000 h^{-1}
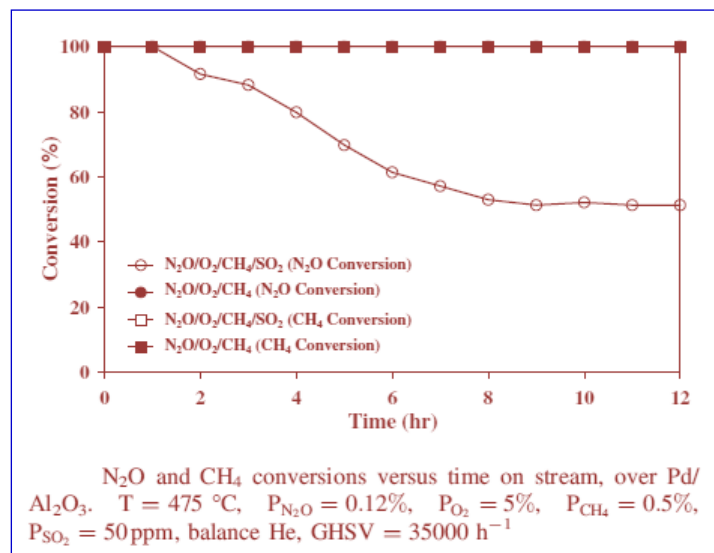
Figure 8: Effect of CO, H_2O and SO_2 on the Activity and Stability of Pd/Al_2O_3 [7].

The presence of reducing agent is going to accelerate the removal of oxygen ad-atoms from the catalyst surface, originated either by N_2O decomposition or gas phase oxygen dissociative adsorption; this in turn can lead to enhanced catalytic activity at lower operation temperatures. In order to be comparable, the feed concentration of reducing agents was appropriately selected in order to obtain a constant C/N_2O ratio. Therefore, propane concentration was kept constant to 0.17% (Figure 7), while the equivalent concentration for CH_4 equaled to 0.5% (Figure 7). It is clearly shown that the presence of reducing agents enhanced the catalytic activity under lean reaction conditions, with C_3H_8 being more efficient than CH_4, especially at lower temperatures. Another major agent that reduces the catalytic activity is the presence of automotive exhausts

Paschalia Taniou, Zoe Ziaka, and Savvas Vasileiadis

containing several other gases leading in deactivation of the catalyst. Figure 8 is presenting a picture at 350 $^{\circ}$C, of the achieved N_2O conversion over Pd/Al_2O_3 (one of the most efficient catalyst in this study) for various feed compositions that contained CH_4, C_3H_8, CO, SO_2 and H_2O. It is clear that the addition of a reducing agent increases the activity. While in the cases of CH_4 and C_3H_8 the performance is slightly increased, CO seems to boost up the N_2O conversion at much higher values. When SO_2 was added, the reaction is inhibited, especially in the case when C_3H_8 was used as a reducing agent. This negative effect was also clear in the case of CO, however when CH_4 was employed this specific inhibition was limited.

Carbon monoxide definitely increases N_2O conversion, while H_2O and SO_2 are clearly deactivated the catalyst. Thermal stability tests in the presence of SO_2 over $Pd–Al_2O_3$, indicate a gradual irreversible decrease in activity, which was due to the formation of surface sulphates (Figure 9).
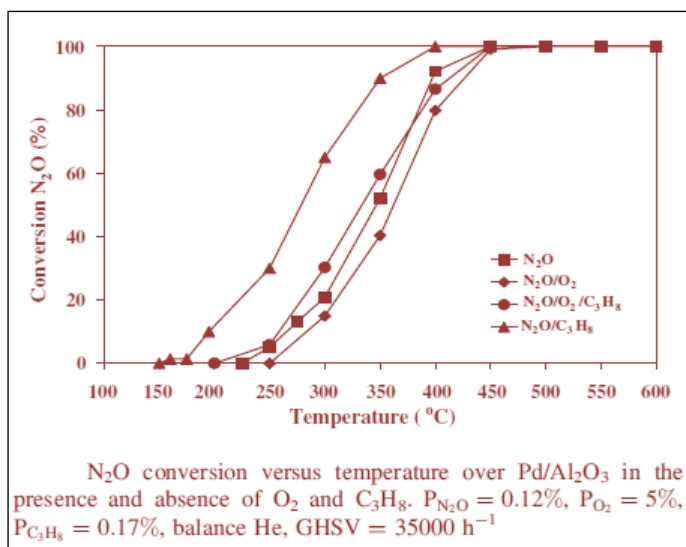

N_2O and CH_4 conversions versus time on stream, over Pd/Al_2O_3. T = 475 °C, $P_{N_2O} = 0.12\%$, $P_{O_2} = 5\%$, $P_{CH_4} = 0.5\%$, $P_{SO_2} = 50\,ppm$, balance He, GHSV = 35000 h^{-1}

Figure 9: Effect of CO, H_2O and SO_2 on the Activity and Stability of Pd/Al_2O_3 [7].

Application.

Among all catalysts tested, noble metals (Pd, Ru, Rh) followed by $Cu–Al_2O_3$ exhibit the best catalytic performance, independently of the experimental conditions imposed. In Figure 10 it is shown that a ca.100% conversion of N_2O is achieved over Pd/Al_2O_3 at 400 $^{\circ}$C in the presence of O_2. This is the best catalytic behavior over a series of noble and transition metal catalysts (Pd, Rh,

Ru, Cu, Fe, In and Ni), supported on γ-Al_2O_3 carrier.

N₂O conversion versus temperature over Pd/Al₂O₃ in the presence and absence of O₂ and C₃H₈. P_{N_2O} = 0.12%, P_{O_2} = 5%, $P_{C_3H_8}$ = 0.17%, balance He, GHSV = 35000 h⁻¹

Figure 10: Best catalytic behavior [7].

Although Pd–Al₂O₃ exhibited the best performance, its activity at low temperatures and H_2O + SO_2 resistivity should be improved additionally (e.g., promotion with alkalis), in order to be considered as a potential solution for mobile exhaust gas treatment applications. [7]

Best case study 2: N$_2$O decomposition over FeZSM-5.

In the last decade, attention was drawn to development of new methods for the abatement of N_2O. Transition metal-exchanged silicon-rich zeolites are excellent candidates for the decomposition of nitrous oxide to nitrogen and oxygen [8]-[15].

Catalyst.

The decomposition of N_2O on zeolite catalysts has been studied extensively. The large surface area and the simultaneous presence of Bronsted positions of the metal centers, contribute to the high performance of M-zeolites, where M = Cu, Fe, Co, etc., perovskite oxides and supported precious metals such as Pd, Rh.

Dominant zeolite systems are iron and copper on zeolite structures (ZSM-5, MFI, BEA, BETA).

Paschalia Taniou, Zoe Ziaka, and Savvas Vasileiadis

In this case study in order to investigate the N_2O decomposition was used the Fe/ ZSM-5 catalyst.

Material and Reaction System.

H. Xia et al. investigated in 2009 the N_2O decomposition through the Fe/ ZSM-5 catalyst, promoted by NO [10]. The experimental procedures were conducted on laboratory space, the gas is a mixture of pure N_2O and with impurities consisting of oxygen. The Fe/ZSM-5 catalysts were synthesized by solid-state ion-exchange method. The as-synthesized sample was calcined in O_2 flow at 823 K followed by the treatment in He flow at 1173 K for 2 h. The content of Fe in the catalyst is about 2.2 wt.%, corresponding to Fe/Al = 0.61. A single-pass plug-flow quartz reactor with an inner diameter of 4 mm was used to test the catalyst performance of Fe/ZSM-5 samples for N_2O decomposition. The catalyst sample (50 mg) was retained between two quartz wool plugs. Prior to N_2O decomposition at a given temperature, the catalyst was pretreated in He flow at 1173 K for 1 h. During transient and steady-state catalytic measurements, the concentration of N_2O was 5.0 vol.% and the gas hourly space velocity was kept at 24,000 ml/g h. For N_2O decomposition in the presence of NO, the gas hourly space velocity was kept at 24,000 ml/g h and the concentrations of N_2O and NO were 5 vol.% and 1 vol.%, respectively. It should be noted that the feeds contain trace amount of water (about 1–10 ppm). To identify the characteristics and the catalytic properties, the following methods were used: XRD, SEM, ICP, TPD, XANES, FTIR, EDX, BET, DRS, Mossbauer spectroscopy, UV-vis spectroscopy and Infrared spectroscopy.

For the best performance of the catalysts, nitric oxide boosters, silver, platinum, cobalt and the reducing agent ammonia (Selective Catalytic Reduction) were also used.

Analysis.

Figure 11 shows the decomposition of N_2O on Fe/ZSM-5 as a function of temperature in the absence and in the presence of NO.
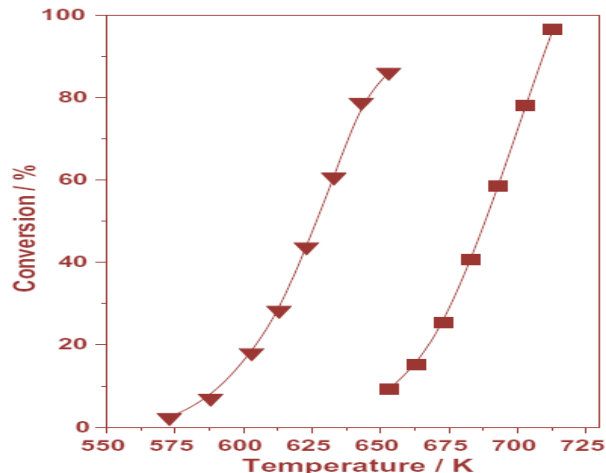
Figure 11: Catalytic Decomposition of N2O in presence (▼) and absence (■) of NO [10].

In a N_2O/He feed, the catalyst presents a substantial N_2O conversion only above 643 K. The presence of NO (NO/N_2O = 0.2) significantly increases the activity of N_2O decomposition. The N_2O conversion curve is shifted to a temperature about 60 K lower for the same conversion. In addition, the addition of NO in the feed leads to a significant decrease in the apparent activation energy.

### *The role of NO as a promoter of the catalytic activity:*

- The presence of NO regenerates the active sites of the catalyst and accelerates the reformation-(recombination) of oxygen during the catalytic decomposition of N_2O.

- plays an important role in the transport and storage of surface oxygen atoms and the fast desorption of O_2.

- helps the Fe^{+3} transformation to Fe^{+2}, releasing O_2 and H_2O, which are the active sites of the catalyst on which the split of N_2O takes place.

N_2O decomposition on Fe/ZSM-5 in the absence and in the presence of NO

The experimental performance after N_2O decomposition reaches a steady-state. The desorption of O_2 always delays more than that of N_2, but at lower temperature during N_2O decomposition; the desorption of N_2 and O_2 are almost synchronic in the presence of NO. This result unambiguously shows that the presence of NO enhances the desorption of O_2 during N_2O direct decomposition.

Paschalia Taniou, Zoe Ziaka, and Savvas Vasileiadis

The concentrations of N_2 and O_2 first reach to their maximum and then decay to a steady-state. Some surface oxygen atoms are deposited on the catalyst due to trace amount of water in the feed. After N_2O decomposition reached a steady-state, a switch from N_2O to NO is performed. In addition of methane and H_2O, the addition of NO could remove hydroxyl groups bound to Fe species. The presence of NO removes the hydroxyl groups bound to the Fe species during the N_2O direct decomposition.

As an indicative explanation for the role of NO in N_2O decomposition, schematic description of catalytic cycles is shown in the Figure 12.
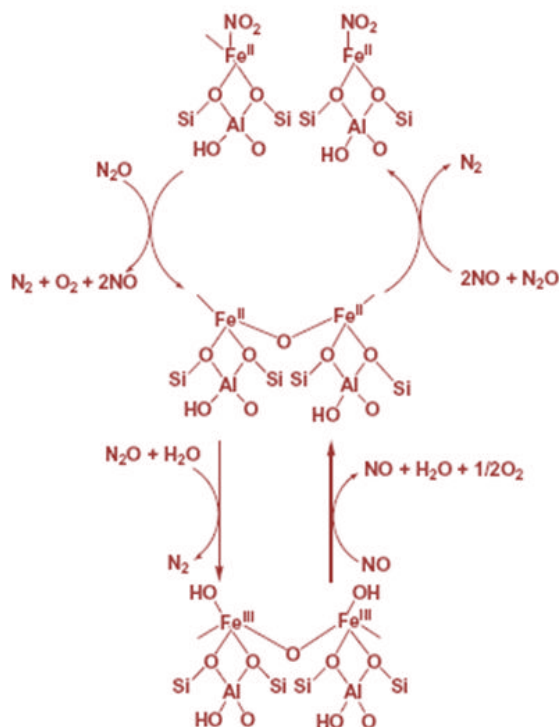
Figure 12: Schematic description of the NO role in N_2O decomposition [10].

The Figure 12 shows the results from in situ spectroscopy and transient response method study, for the first time. Bi-nuclear Fe sites are proposed to be the active sites for the NO-assisted N_2O decomposition.

In addition, the role of water in the structural transformation between the dehydroxylated and the hydroxylated bi-nuclear Fe sites was also elucidated. We conclude that the NO_2 species adsorbed on binuclear Fe sites could be an intermediate species in N_2O decomposition in the presence of NO. The two adjacent NO_2 adsorbed on the bi-nuclear Fe sites could react with each

* Corresponding author (Z. Ziaka). Tel/Fax: +30-2310-275473 E-mail addresses: bookeng@hotmail.com, z.ziaka@ihu.edu.gr.

other to release O_2, or the adsorbed NO_2 species could react with N_2O to release O_2.

It has been presented that the structure of the Fe species in Fe/ZSM-5 is strongly dependent on the synthesis method, zeolite precursor, amount of Fe loading, and pretreatment conditions.

Application

The best performance (about 90%) in the decomposition of N_2O was observed by using the catalyst Fe-ZSM-5, at 583K (310^oC) in the presence of NO.

Zeolites iron is more prevalent; however the problem is that at low concentrations of Fe they do not show good catalytic behavior, while, when the concentration is high, they show good catalytic activity only at high temperatures. The copper zeolites are promising catalytic systems in the reaction of N_2O decomposition and especially amorphous oxide systems that contain copper (based on CuO_x). These are characterized by high mechanical and hydrothermal stability.

Best case study 3: Excellent catalytic performance of $Zn_xCo_{1-x}Co_2O_4$ spinel catalysts for the decomposition of nitrous oxide.

Currently, oxide spinels of 3d transition metals have been shown an increasing fundamental and applied research activity because of their special electric, magnetic, and catalytic properties. Spinel oxides belong to a class of complex oxides with the chemical formulas of AB_2O_4 in which A ions are generally divalent cations occupying tetrahedral sites and B ions are trivalent cations in octahedral sites. The cobalt oxide spinel Co_3O_4, for example, is the one receiving considerable interest [16]-[24]. Regarding their applications in catalysis, for example, it has been proved that the catalytic activity of these spinels depends essentially on two actors: the degree of substitution and the inversion degree of the spinel.

Catalyst

During the catalytic decomposition of N_2O, using the spinel $Zn_xCo_{1-x}Co_2O_4$, the cobalt ions replace Co^{+2} ions with Zn^{+2}. The activity of the catalysts was found to depend on the degree of this substitution. L. Yan et al., investigated the role of this substitution and presented the best catalytic performance for the N_2O decomposition until nowadays. [17]

Paschalia Taniou, Zoe Ziaka, and Savvas Vasileiadis

Materials and Reaction System

The catalytic preparation was based on co-precipitation method, adding aqueous solution of K_2CO_3 (15 wt%) in a mixture of aqueous solutions $Co(NO_3)_2$ and $Zn (NO_3)_2$ to produce the $Zn_{0.36}Co_{0.64}Co_2O_4$ catalyst.

Before the catalytic experiments, 0.6 g catalyst was pretreated for 30 min by 20% oxygen in He at 400 ^{o}C in order to remove the organic compounds adsorbed on the surface of samples, then decreased to reaction temperature. The catalytic reaction was carried out in a standard fixed-bed flow reactor by passing a gaseous mixture of N_2O (1000 ppm), 0 or 10 vol% O_2, 0 or 5 vol% H_2O in a He flow rate 100–150 ml/min to get a space velocity of 15,000 h^{-1}. To get reliable N_2O conversion, the reaction system was kept for 30 min at each reaction temperature, then it started to analyze the off-gases with two on-line gas chromatographs.

Table 5 shows the characterization results, the conversion and reaction rate of N_2O at 200 ^{o}C of the samples of different degree of Co^{2+} substitution by Zn^{2+}.

Table 5: The characterization data of the catalysts

Catalyst formula[a]	BET surface area[b] (m^2/g)	Conversion of N_2O [c] (%)	Rate of N_2O conversion[b] (x10^6 mol/g s)
$Co_3 Co_4$	56.6	1.6	0.12
$Zn_{0.36} Co_{0.54}Co_2 O_4$	73.6	98.4	7.31
$Zn_{0.54} Co_{0.46}Co_2 O_4$	76.2	90.2	6.71
$Zn_{0.70} Co_{0.30}Co_2 O_4$	75.1	84.0	6.25
$Zn_{0.98} Co_{0.02}Co_2 O_4$	72.8	60.1	4.46
1.1% Au/ $Co_3 O_4$	23.6	22.6	4.04

[a] Determined by AAS method.
[b] Characterized with ASAP 2010.
[c] Determined at 200 ^{o}C.

Analysis

Catalytic decomposition activity for N_2O

The conversion of N_2O to N_2 and O_2 over $Zn_xCo_{1-x}Co_2O_4$ spinel oxides at 200°C (shown in Table 5) indicated that the introduction of Zn into the spinel structure of Co_3O_4 led to a significant improvement (conversion of N_2O from 1.6% over pure Co_3O_4 to 98.4% over $Zn_{0.36}Co_{0.64}Co_2O_4$ at

200°C) in catalytic activity for N_2O decomposition. Then with increasing the x value, the catalytic activity of samples decreased slowly (conversion of N_2O decreased from 98.4% at x = 0.36 to 60.5% at x = 0.98).

On the weight basis of catalyst, the $Zn_xCo_{1-x}Co_2O_4$ catalysts gave much higher activity than that of pure Co_3O_4. Moreover, on the basis of surface area of catalysts, $Zn_xCo_{1-x}Co_2O_4$ samples still are more active. For instance, when comparing the N_2O conversion of the $Zn_{0.36}Co_{0.64}Co_2O_4$ sample with conversion of pure Co_3O_4 at 200 °C, it is clear that the specific activity (per square meter of catalyst) is still much higher over the $Zn_{0.36}Co_{0.64}Co_2O_4$ catalyst. Compared to the rate (Table 5) of N_2O decomposition of 1.1% Au/Co_3O_4, the rate of $Zn_{0.36}Co_{0.64}Co_2O_4$ is higher, which indicated that the $Zn_xCo_{1-x}Co_2O_4$ catalysts were more active than that of 1.1% Au/Co_3O_4 for direct N_2O decomposition reaction.
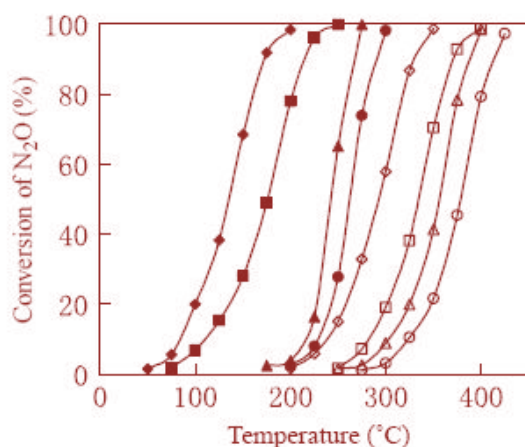
Figure 13: The effect of gas composition on N_2O conversion at the space velocity of 15,000 h^{-1}. Gas composition (◊,◆), 1000 ppm N_2O; (□, ■), 1000 ppm N_2O+10% O_2, (Λ, ▲), 1000 ppm N_2O+5% H_2O; (○, ●), 1000 ppm N_2O+10% O_2 +5% H_2O in He. The open symbols refer to CO_3O_4, and the closed symbols to the $Zn_{0.36}Co_{0.64}Co_2O_4$ catalysts [17].

N₂O decomposition in the presence of excess O₂ and H₂O

The presence of excess O_2 has a moderate degree of inhibition of the degradation of N_2O, which indicates that the N_2O and the O_2 competes for adsorption on the active sites of the catalyst.

The presence of water, however, severely inhibited the reaction of decomposition of N_2O, possibly due to the hydroxylation of active sites and the adsorption of these. As the temperature increases, water is desorbed from the surface active sites and dehydroxidate thus increasing the efficiency of the N_2O decomposition. Although the presence of excess O_2 and water inhibited the

reaction, the conversion of N_2O reaches up to 100% even in the presence of 10 vol % O_2 and 5 vol % water at 300 °C.

Figure13 shows the effect of the presence of excess O_2 and H_2O on catalytic activity over $Zn_{0.36}Co_{0.64}Co_2O_4$ and pure Co_3O_4.

As the temperature increased, water was desorbed from the surface active sites and the active sites dehydroxylated, the conversion of the N_2O decomposition increased sharply. The influence of hourly space velocity on the catalytic performance of $Zn_{0.36}Co_{0.64}Co_2O_4$ at 200°C and the temperature of 100% N_2O conversion (T100) was also carried out in the Figure 14:
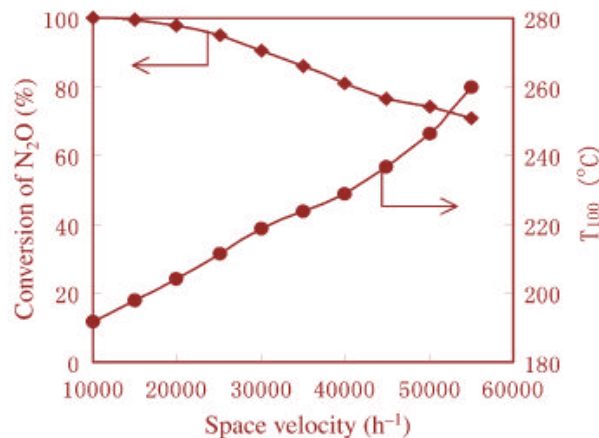
Figure 14: The effect of space velocity on the conversion of N_2O at 200°C and T100 (the temperature of 100% N_2O conversion) over $Zn_{0.36}Co_{0.64}Co_2O_4$ catalyst [17].

The results indicated that the conversion of N_2O slowly decreased with increasing of space velocity. The N_2O conversion reached 100% and 71.3% at the space velocity of 15,000 and 55,000 h^{-1} at 200°C, respectively. The temperature of 100% N_2O conversion was 263 °C at a space velocity of 55,000 h^{-1}. It indicated that the $Zn_{0.36}Co_{0.64}Co_2O_4$ spinel oxide is highly active for N_2O decomposition reaction and can be operated at a relatively higher space velocity.

Application

The present results have demonstrated that the introduction of Zn into the spinel structure of

Co_3O_4 significantly promoted the catalytic activity for N_2O decomposition.

The yields are shown in the table 6 at various conditions.

Rh- or Ru-exchanged zeolites and calcined hydrotalcites are the best catalysts for N_2O decomposition in literature. Compared to the catalysts (Table 6), $Zn_{0.36}Co_{0.64}Co_2O_4$ catalyst is more active for N_2O decomposition reaction under similar reaction conditions.

Table 6: Comparison of catalytic activity of $Zn_{0.36}Co_{0.64}Co_2O_4$ with the best catalysts in literature for N_2O decomposition.

Catalyst_formula[a]	200 ^oC	250 ^oC	300 ^oC	350 ^oC	400 ^oC	450 ^oC
	N_2O conversion %	N_2O conversion %	N_2O conversion %	N_2O conversion %	N_2O conversion %	N_2O conversion %
$Zn_{0.36}Co_{0.64}Co_2O_4$[a]	72(35[b])	98(59[b],8[c])	100(91[b],57[c])	100(100[b],98[c])	-	-
Co-Rh-Al-HT[d]	-	-	100(7[f])	-	100(67[f])	100(100[e],100[f])
Rh(Ru)-ZSM-5[d]	-	20	74	98	-	-

[a] Test conditions:1000ppm N_2O in He, GV = 55,000 h^{-1}.
[b] With 10% oxygen.
[c] . With 10% oxygen and 5% water.
[d] 990 ppm N_2O in He, GV = 60,000 h^{-1}
[e] With 2.5% oxygen
[f] With 2.5% oxygen and 2.5% water

The appropriate catalyst is prospective to be used in practice for the removal of N_2O.

Best case study 4: Mullite-supported Rh catalyst.

For rhodium catalysts, oxygen desorption is generally considered as the rate limiting step in related reactions of NO_x. In this case study it was investigated the decomposition of N_2O over rhodium catalysts [25]-[29]. Many of them suffer from inhibition by oxygen. Different theories exist to explain the fact that rhodium catalysts can decompose N_2O effectively in oxygen-rich feeds, but are rapidly deactivated because of the saturation of the active centers by adsorbed oxygen.

Catalyst

From the Rh-team catalysts for the N_2O decomposition the most widely used, commercially available, is the one supported on γ-Al_2O_3.

Paschalia Taniou, Zoe Ziaka, and Savvas Vasileiadis

The activity of the catalyst depends largely on the properties of the carrier, as the γ-Al_2O_3 contains different amounts of Na ions, different each time modifying the crystalline structure of the surface, thus affecting the active phase of catalyst. During the decomposition of N_2O mechanism, the desorption of O_2 is the limiting step of this reaction and it has emerged that is a deterrent function of rhodium catalysts, and created strong beams-Rh, blocking the active sites.

X. Zhao et al. in 2009 investigated the activity of a promising material for the N_2O decomposition due to its capacity to survive in the required high temperature environment or capable to initiate decomposition at low enough temperatures [29]. So a novel catalyst was designed by supporting rhodium on mullite, with the aim of developing a practically capable catalyst for N_2O used as a propellant, and probing into the role of mullite. Rhodium was chosen as the active component for the reason that Rh has exhibited excellent activities for the abatement of N_2O at low concentration [29].

### Materials and Reaction System

Mullite is a ceramic material with excellent thermal and mechanical properties: high porosity, thermal stability and unusual crystalline structure. The porous structure can be easily achieved by incorporating appropriate factors or through the decomposition of $Al(OH)_3$ during the manufacturing process. The oxygen vacancies are abundant due to the balancing of double substitution of Si^{+4} and Al^{+3}. Mullite synthesized by $2SiO_2.3Al_2O_3$ using commercial Al $(NO_3)_3$ and (TEOS: tetraethylorthosilicate) calcinated at 1473 K (Rh / M). The alumina prepared by Al_2O_3, calcinated at 773 K (Rh/Al). The Rh content was 5 wt%. For the catalytic preparation wet impregnation and ignition was used at 1473K: [Rh / M-HT] and [Rh / Al-HT].

The catalytic performance of N_2O decomposition was evaluated in a fixed bed flow reaction system. The reacting gas contained 30 v/v% N_2O in Ar, and was introduced at a flow rate of 50 mL min^{-1}, corresponding to a gas hourly space velocity of 30 000 mL g^{-1} h^{-1}; and the catalysts were reduced with H_2 at 773 K for 2 h before reaction.

Analysis

Figure 15 compares the catalytic activities of different catalysts as a function of reaction temperature. As expected, the Rh/M catalyst exhibited a superior high activity in N_2O.
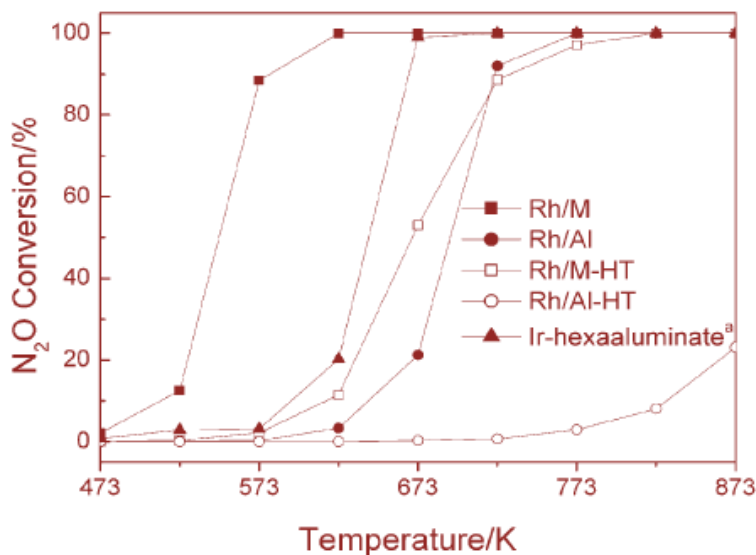
Figure 15: N_2O decomposition on Rh-catalysts [29].

For the Rh / M case: The catalytic activity starts at 473K and at the temperature of 573 K (300^oC) achieved the 90% conversion. For the Rh / Al case, the 100% conversion achieved at 773 K while the active surface is 5.7 times greater than that of Rh / M, the rhodium content is the same for both types of catalysts. The good catalytic performance of Rh / M is related to the mechanism of decomposition of N_2O. In the second step of the mechanism of the decomposition of N_2O, N_2O decays via the redox mechanism of oxygen desorption from the catalyst surface. In this catalyst, there are many places covered by oxygen, which may indicate that the adsorption of oxygen is related to the structure of mullite where the loads balanced on a Si^{+4} and Al^{+3}.

The extra ignition in catalyst at 1473 K shows lower activity, which is associated with the change of crystal structure and the gasification of Rh compounds [29].

In Figure 15 the catalytic activities of different catalysts are compared as a function of reaction temperature. As expected, the Rh/M catalyst exhibited a superior high activity in N_2O decomposition. The Rh/Al sample also showed a good activity, decomposing N_2O completely above 773 K. The BET surface area of the Rh/M is 5.7 times lower than that of the Rh/Al, while the Rh contents were approximately equal. But the BET surface area and the active component content are not primary parameters for the Rh/M. The superior activity of the Rh/M can also be confirmed by comparing its activity with that of the Ir-hexaaluminate catalyst as plotted in the Figure. The catalysts calcined at 1473 K demonstrated a significant decrease in the N_2O

Paschalia Taniou, Zoe Ziaka, and Savvas Vasileiadis

decomposition reactivity. However, the Rh/M-HT activity was decreased relatively little, revealing its fairly good thermal stability after high-temperature calcination, while the Rh/Al-HT exhibited almost zero activity after calcining at 1473 K. The drastic decrease in N_2O conversion of the Rh/Al-HT is believed to be correlated with the distinct crystal transition and serious volatilization of Rh species. Moreover, mixed Al_2O_3–SiO_2 oxides with the same Al/Si ratio as mullite were also synthesized with the same procedure. The Rh/AS catalyst exhibited a similar activity as that of Rh/Al, while Rh/AS-HT showed only a minimal decease in activity. This can be explained by the formation of the mullite structure.

Application

The best catalytic behavior is presented by the Rh / M: at the temperature of 573 K (300 ^{o}C) achieved the 90% conversion of N_2O.

However, the existing catalysts for the N_2O decomposition have been found to be either unsurvivable in the required high-temperature environment or unable to initiate decomposition at low enough temperatures. The novel catalyst mullite-supported Rh is highly desirable to be more active and stable to trigger the decomposition of N_2O.

Innovative case study: N_2O-mediated propane oxidative dehydrogenation over Fe-zeolites.- TEOM studies for continuous propylene production in a cyclically-operated reactor.

Steam-activated iron-zeolites (FeZSM-5, Fe-silicalite, Fe-beta) are highly efficient catalysts for the oxidative dehydrogenation of propane using N_2O, with initial propylene yields up to 25% at 723 K, but they deactivate due to coking. Since catalyst deactivation is reversible, the feasibility of a cyclically-operated process for continuous propylene production, with alternation of reaction and regeneration cycles, has been analyzed. In order to rationally design the sequence in the cyclic experiments, a tapered element oscillating microbalance (TEOM) coupled to on-line analysis of products has been applied. The TEOM provides information on activity, deactivation, and regeneration by simultaneous measurement of reaction and mass changes. In a system with two fixed-bed reactors in parallel using FeZSM-5, stable propene yields higher than 20% were obtained during cycling for 2000 min, using reaction and regeneration temperatures of 723 and 823 K,

respectively. This catalytic process leads to the simultaneous valorization of C_3H_8 and N_2O and can be economically applied for on-site propylene production using a low-cost source of N_2O, e.g. in tail-gases of chemical processes where N_2O is produced in high concentration [30].

$$C_3H_8 + N_2O \rightarrow C_3H_6 + N_2 + H_2O$$

Propylene production is very important for further production of polypropylene.

The above reaction is essential not only for the reduction of N_2O but also for propylene and polypropylene production, both of them used in large amounts in the petrochemical and plastics industry.

By further introduction to a membrane separation of N_2 in the production side more and more propylene is going to be produced.

It is also useful to possibly utilize a membrane reactor so that to combine both separation and reaction in one step for better improvements and economical outcomes [43], [44].

Polyolefins such as polypropylene (PP), polyethylene (PE) and their copolymers, poly(butene-1), polyisobutylene, poly(4-methylpentene-1) are high value commodity polymers. They are produced in high capacity annually and used in manufacturing of plastics, medical/industrial parts and tools, chemicals, and household products. Polypropylene alone has a production capacity of about 8.5 million m.t. annually in North American and 44 million m.t. globally. Polyethylene has a higher global capacity in annual production. Both are predicted to grow in the years to come.

The new process proposed here uses the permeable reactor concept (membrane reactor or permreactor) in order to design a catalytic dehydrogenation membrane reactor (CDMR) of paraffins (alkanes) to olefins (alkenes). The process integrates the CDMR with a polymerization reactor (PR) (gas phase or slurry type) for polyolefin production in a two step reactor process. A third vessel, a separator (or permeator) complements the flow chart to separate, in gas phase, the unreacted olefin from the paraffin at the exit of the polymerization reactor. Olefin (e.g., propylene) is fed back into the PR inlet and the paraffin (e.g., propane) is recycled into the CDMR inlet. Thus, the entire process consists of an integrated reaction-separation-recycling system for the production of polymer grade olefins and subsequently of polyolefin products through a first step

Paschalia Taniou, Zoe Ziaka, and Savvas Vasileiadis

catalytic dehydrogenation process of paraffin-feedstocks.

Production of polymer grade olefins through polymerization reactions usually requires pure monomers as feedstocks to avoid catalyst and solvent contamination and rapid loss of catalyst activity during polymerization. Depending on the type of the downstream utilized polymerization reactor and process (e.g., solution, bulk, suspension, emulsion, gas phase) and the type of the polymer chain propagation reactions (i.e., step-reaction, radical-chain (addition), ionic, coordination) the purity, flowrate and concentration of the monomers (olefins) may vary in the reactor feed. These feed parameters for the monomer are coupled with the polymerization temperature, pressure and reactor volume to make for the production of specific polymers within the desired range of molecular weight, structure and properties (i.e., crystallinity, transparency, viscosity, tensile and impact strength). Specifically, most of the aforementioned commercially available polyolefins are produced with coordination type polymerization and catalysts. Both stirred bed (slurry-multiphase type) reactors and fluid bed (gas phase type) reactors can be used in coordination polymerization employing coordinated complex catalysts (of Ziegler-Natta type) or supported metal oxide catalysts.

Hydrocarbon type solvents are used in the slurry process (e.g., hexane, heptane). Commercially established reactors and reactor modifications of both types operate at conditions which usually range from T=50 to 250 °C and P=1 to 30atm. The exothermic heat of the polymerization reaction is removed by cooling the reactor externally or internally (i.e., by vaporizing a suitable solvent or diluent) or by circulating the unreacted gas through external cooling devices. The above described coordination type polmerization reaction can utilize hydrogen product from the CDMR within the reactor as a chain transfer agent to reduce the polymer molecular weight (MW) and achieve branching which contributes to a decreased crystalline product wherein such an end polymer is required.

Moreover, the olefin monomer can be diluted with a paraffin or cycloparaffin during the polymerization in both types of reactors mentioned above. The proposed processes seek to utilize as part of the diluent or solvent in polymerization reactor the unreacted (non-consumed) paraffin from the CDMR (e.g., propane for polypropylene, ethane for polyethylene, n-butane for poly(butene-1, etc.) to increase the process efficacy and economy. The unreacted paraffins can

remove the exothermic heat of polymerization by vaporization at the reaction conditions. As an example, propane and propylene have low boiling points and under usual polymerization conditions (25-35atm, 55-70°C) they can be transferred from the liquid to the gas phase through boiling.

Mixing with a higher paraffin such as hexane or heptane in the slurry process is also possible in order to increase the solvent efficiency towards the formed polymer and promote mixing in the reactor. By utilizing propane in polypropylene reactor, the propane/propylene separation cost before polymerization can be eliminated.

Furthermore, the use of propane or the corresponding higher carbon paraffins (e.g., butane, pentane) as solvents in polymerization, minimizes the use of higher priced organic solvents and provides an environmentally benign process modification. However, the non-utilized propane or higher carbon paraffins exiting from the PR have to be recycled into the CDMR in order to keep the operation cost low and the continuous production of propylene or higher olefin monomers as shown in Figure 16. Thus, the solvent-like initial paraffin needs to be separated from the unreacted olefin at the top exit of the polymerization reactor.

The proposed separator/permeator (E) as shown in the flow chart of the Figure can operate based on dense or nanoporous solid type polymer reactive membranes, or liquid membranes, containing activated metal ions such as Cu (copper), Ag (silver), Zn (zinc), Cr (chromium), Fe (iron), Ni (nickel), Co (cobalt). These ions have a degree of affinity to form a transporting complex with the permeating olefin (e.g., propylene, ethylene) and to facilitate its transport via the membrane. Moreover, facilitated transport of olefins via metal coated and metal-ion exchange membranes can be also used as separation candidates in separator E.

The described membrane based separation processes compete well energetically and economically with currently applied separation techniques such as the low temperature hydrocarbon distillation.

Furthermore, our long term goal is the development of more stable membranes to perform this separation. Such new membranes can be based on composite metal-polymer, metal-inorganic, or polymer-inorganic materials, stable at higher temperatures and pressures for the separation of

Paschalia Taniou, Zoe Ziaka, and Savvas Vasileiadis

olefins [44].
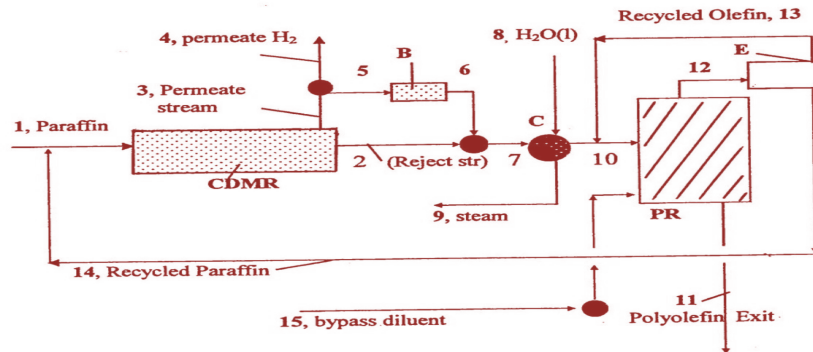
Figure 16: Flow sheet of integrated olefin/polyolefin production in a membrane reactor [43, 44]
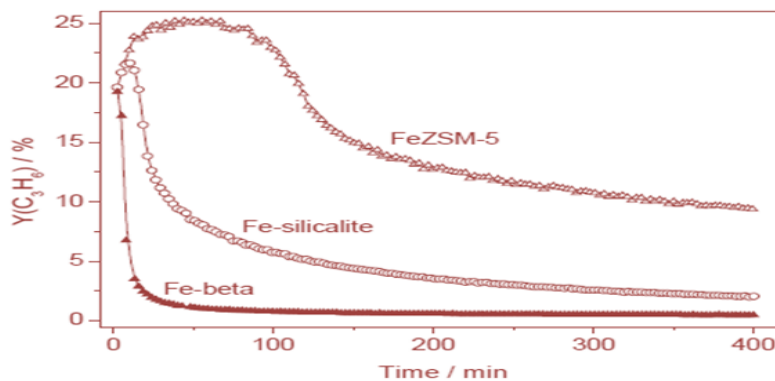

Figure 17: Coke content and C_3H_6 yield vs. time during ODHP with N_2O over steam-activated Fe-zeolites at 723 K. Conditions: 100 mbar C_3H_8 and 100 mbar N_2O in He, WHSV = 400, 000 ml h^{-1} g^{-1}_{cat}, and P = 2 bar [30].

- The initial propylene yield was about 19-22% at 723K, with a degree of conversion of about 45% propane and propylene selectivity of about 50%, with complete conversion of N_2O.

- The interaction of C_3H_8 with N_2O through iron zeolites (O_2 absence) does not lead to propylene production, underlining the essential role of oxygen in this dehydrogenation.

  The conversion of N_2O at 673K is 15%, 25% at 723K and 75% at 773K.

  The adsorbed atomic oxygen plays an important role in the regeneration of zeolite and in the oxidation of coke.

- In conclusion: the cyclical process of continuous production of propylene by N_2O ODHP through Fe-zeolites is extremely effective for the oxidative dehydrogenation of propane, but deactivated due to coke formation. The deactivation process is greatly influenced by the type of host zeolite and the reaction temperature.

- The propylene-N_2O process competes with a number of other processes for propylene production such as the dehydrogenation of propane in a membrane reactor described above.

2.1.1 N_2O Decomposition through membrane

Measurement and analysis of gas permeability in polymeric membranes is an important research tool in a proper design and selection of operating conditions for a gas separation system. Measurement results produce variations in species permeability as a function of feed composition, driving pressure, temperature and membrane type [31]-[36].
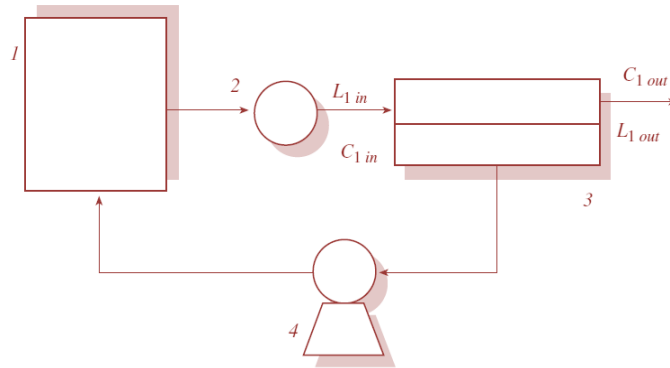
Figure 18: A typical schematic presentation of N_2O decomposition through membranes [34].
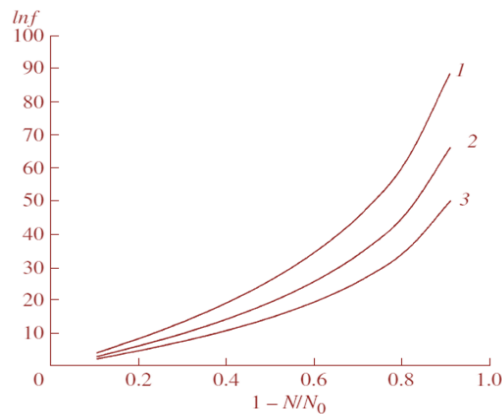
Figure 19: The dependence of separation degree from sampling rate for nitrous oxide – oxygen, $1 - L_{1\,in}/L_{1\,out} = 100, \quad 2 - L_{1\,in}/L_{1\,out} = 70, \quad 3 - L_{1\,in}/L_{1\,out} = 50$ [34].

Membranes are promising materials during the N_2O decomposition and separation, their utilization is not only of interesting because of their ecological aspect but also because of their economical method due to their low cost. Such an example, characterized by low consumption of both materials and energy, is represented below through the Figure 18.

Paschalia Taniou, Zoe Ziaka, and Savvas Vasileiadis

The dependence of separation degree of nitrous oxide from nitrogen and oxygen at different values of feed and flows ratios is presented in Figure 18, respectively.

As it is shown in Figure 19, it is possible to achieve high purity level of nitrous oxide even at small sampling rates. For example, at sampling rate equal to 15%, the concentration of oxygen impurity for the system nitrous oxide – oxygen is decreasing more than 1000 times. As a result, the oxygen concentration is satisfying the purity requirements. And for the system nitrous oxide – nitrogen, the purity requirement is met at a lower sampling rate (not more than 10%).

It was shown that a membrane module with a feeding reservoir might be effectively used for nitrous oxide high purification from nitrogen and oxygen at room temperature and with small product losses [34].

Table 7: Calculated selectivities of nitrous oxide–gas system for various polymer membranes, determined as ratio of permeabilities.

Membrane type	α: N_2O-O_2	α: N_2O-N_2	α: O_2-N_2	$P \times 10^{14}$, mole m/(m^{2}sPa)
Lestosil (present work)	5.0 ± 0.2	10.1 ± 0.4	2.0 ± 0.01	98.6 ± 2.8
Silicon rubber	109	-	-	204
Cellulose acetate	6.3	30.4	4.8	592
Polydimethilsiloxane	7.2	15.5	2.1	145.9
Perfruoro(2-methylen-4-methyl-1,3-dioxocyclopenante)	0.5	2.2	4.4	7.0
Poly[bis(triflouroethoxy) Phosphazene]	6.1	14.6	2.4	72

As a membrane module in this case, a commercially available composite non-porous polymeric membrane named "Lestosil" was used, which base is a staircase copolymer of poly(dimethylsiloxane) and poly(diphenylsiloxane). The thickness of the membrane was 5μm.

For permeability measurements a manometric method was used. The values of permeability coefficient were measured for nitrous oxide, nitrogen and oxygen at feed pressure in the range from 10^5 to 4×10^5 Pa. The value feed pressure was increased and then decreased stepwise. The experimental results and calculated selectivities of the nitrous oxide gas system, determined as ratio of permeabilities, are presented in detail in the Tables 7 and 8.

Table 8: Ideal selectivity at different feed pressures.

$p_1 \times 10^{-5}$, Pa	α: N_2O-O_2	α: N_2O-N_2	α: O_2-N_2
1.0	5.0 ± 0.2	10.0 ± 0.7	2.0 ± 0.1
2.0	4.9 ± 0.5	9.8 ± 1.6	2.0 ± 0.3
3.0	5.2 ± 0.6	10.5 ± 1.2	2.0 ± 0.1
4.0	5.3± 0.6	10.7 ± 2.1	2.0 ± 0.3
3.0	5.2 ± 0.6	10.5 ± 1.3	2.0 ± 0.2
2.0	4.9 ± 0.4	9.8 ± 1.1	2.0 ± 0.2
1.0	4.7 ± 0.1	9.5 ± 0.7	2.0 ± 0.2

As it is shown above, the selectivity of systems, consisting of the investigated gases, does not depend on the feed pressure. It is clear that nitrous oxide has the biggest permeability in comparison with its impurity components. In case of one membrane module, the use of the value of enrichment factor is limited to selectivity. Therefore, periodical purification with permeate recycle should be advisably considered to improve the effectiveness of nitrous oxide high purification process. One of the examples of such an operation is the membrane module with a feeding reservoir presented in Figure 18. The purified gas mixture inserts in the feeding reservoir *1* from where it is actually flown at constant pressure, provided by reducer *2* into the high pressure cavity of membrane module *3*. The impurity component is partially removed while the purified mixture which is enriched by the highly permeable component (nitrous oxide) is coming back into feeding reservoir 1 by the vacuum-compressor *4*. Then the process is continuously repeated until to reach a high purity level of nitrous oxide. The separation factor *F* of the process is given by the relationship below:

$$F^{-1} = \frac{C_{1out}}{C_{1in}} = \left(\frac{L_{1in}}{L_{1out}}\right)^{\frac{\alpha^* - 1}{\alpha^*}}$$

(1)

where C_{1in}:   impurity concentration of feed flow of membrane module, ppm;

     C_{1out}:   impurity concentration of retentate flow, ppm;

     L_{1in}/L_{1out}:   ratio of feed and retentate flows of membrane module;

     α^* :   effective selectivity;

The effective selectivity for the low permeable component is defined as:

$$\alpha^* = \alpha - \frac{p_2}{p_1}(\alpha - 1),$$

(2)

where p_1, p_2 are pressure of high and low pressure cavities respectively, in Pa; α: ideal selectivity. The purification degree (f) in this case should be calculated by the following equation:

     Paschalia Taniou, Zoe Ziaka, and Savvas Vasileiadis

$$f = \frac{C_0}{C} = \left(\frac{N_0}{N}\right)^{\frac{1-F}{F}}$$

<div align="right">(3)</div>

where C, C_0 and N, N_0 are the quantity of mixture and its concentration, in the feeding reservoir, before and after purification, respectively.

3. Conclusions

The purpose of this review study is to record catalytic processes of decomposition of N_2O, and propose some innovative solutions that could be investigated and implemented in the future as new technologies. The total contribution of N_2O, because of its long life time, to the greenhouse effect is 310 times larger than that of the combined CO_2 and CH_4 . The proposals therefore, through this work are as follows:

A number of CDM projects is under development globally for the effective decomposition of N_2O and the alleviation of its greenhouse effects.

Pd/Al_2O_3 is the best catalyst among other noble metals for the effective decomposition of N_2O. Oxygen is an inhibitor for the N_2O decomposition reaction while hydrocarbons and especially propane are catalytic promoters.

Zeolites can play an important role in the N_2O decomposition. Research in underway to discover efficient zeolite structures to facilitate this decomposition reaction. Fe/ZSM-5 is a good zeolite catalyst to promote the N_2O decomposition reaction, especially under the presence of NO.

The spinel catalyst $Zn_{0.36}Co_{0.64}Co_2O_4$ offers complete N_2O conversion (up to 100%) at temperatures above 250 ^oC and consists an important class of materials for N_2O decomposition reaction.

The Rh/Mullite catalyst offers an excellent performance in N_2O decomposition. This class of catalysts offers 100% conversion of N_2O at temperatures above 350 ^oC.

The oxidative dehydrogenation of propane on zeolite catalysts is an effective way to reduce N_2O into N_2 with the simultaneous production of propylene. The conversion of N_2O at 400^oC reaches 15%, 25% at 450 ^oC and 75% at 500 ^oC. However, the process is deactivated due to coke

formation. The deactivation is strongly affected by the type of the host zeolite and the reaction temperature.

The last process competes with the dehydrogenation of propane taking place in a membrane reactor for the production of propylene and hydrogen. Propylene is subsequently used in a polymerization reactor for the production of polypropylene. This process uses membranes and recycling streams to achieve its goals of high yields in propylene and polypropylene production.

Membranes of polymer nature can be used in modules for the effective purification of nitrous oxide from nitrogen and oxygen based on the permeability differences of these three components. It is shown that the selectivity of the permeating gases in the polymer system used (Lestosil) does not depend on the feed pressure.

Use of the catalytic membrane reactor concept where the reaction of propane with N_2O takes place. This application can be lucrative in the possible separation of propylene product from propane and the other components in order to have an increased consumption of N_2O.
Thus, the catalytic reaction of propane and nitrous oxide to propylene, provides a double and important application of useful utilization of both N_2O reduction and propylene production for further use as polypropylene feedstock.

The combination of the above findings can be further investigated and perhaps propose new innovative solutions that will benefit both economically and in terms of energy and materials conservation the decay processes of N_2O.

4. Acknowledgements

5. References

[1] "**Catalytic decomposition of N$_2$O**," J. Haber, T. Machej, J. Janas, M. Nattich, Institute of Catalysis and Surface Chemistry, Polish Academy of Sciences, ul. Niezapominajek 8, 30-239 Cracow, Poland, 2004.

[2] "**Nitrogen Cycle**," D. A. Jaffe and P. S. Weiss-Penzias, University of Washington, Bothell, WA, USA, Nitrogen Cycle, Atmospheric, (2003) 431-440.

[3] "**Adsorption and reactivity of nitrogen oxides (NO₂, NO, N₂O) on Fe–zeolites",** M. Rivallan, G. Ricchiardi, S. Bordiga, A. Zecchina, J. Catalysis, 264 (2009) 104-116.

[4] "**A review of the current application of N₂O – Emission reduction in CDM projects",** S-J. Leea, I-S. Ryua, B-M. Kimb, S-H. Moona, International Journal of Green House Gas Control, 1-10, G Model, IJGGC-332.

[5] **"Catalytic decomposition of N₂O over noble and transition metal containing oxides and zeolites. Role of some variables on reactivity".** G. Centi, A. Galli, B. Montanari, S. Perathoner, A. Vaccari, Cataysis Today 35 (1997) 113-120.

[6] **"Experimental research on catalytic decomposition of nitrous oxide on supported catalysts".** Y. Wang, J. Zhang, J. Zhu, J. Yin, H. Wang , Energy Conversion and Management 50 (2009) 1304-1307.

[7] **"N₂O Abatement Over γ-Al₂O₃ Supported Catalysts: Effect of Reducing Agent and Active Phase Nature".** G. Pekridis, C. Athanasiou, M. Konsolakis, I. V. Yentekakis, G. E. Marnellos, Top Catal (2009) 52:1880–1887, DOI 10.1007/s11244-009-9346-6.

[8] **"Chemistry of N₂O decomposition on active sites with different nature: Effect of high-temperature treatment of Fe/ZSM-5"** K. Sun, H. Xia, E. Hensen, R. van Santen, C. Li*, Journal of Catalysis 238 (2006) 186-195.

[9] **"Temperature-dependent N₂O decomposition over Fe-ZSM-5: Identification of sites with different activity"** E. Berrier, O. Ovsitser, E.V. Kondratenko, M. Schwidder, W. Grünert, A. Brückner*, Journal of Catalysis 249 (2007) 67-78.

[10] **"The promotional effect of NO on N₂O decomposition over the bi-nuclear Fe sites in Fe/ZSM-5"** H. Xia, K. Sun, Z. Liu, Z. Feng, P. Ying, C. Li, Journal of Catalysis 270 (2010) 103-109.

[11] **"Metal Exchanged ZSM-5 Zeolite Based Catalysts for Direct Decomposition of N₂O"** S. Kumar, S. Rayalu, N. Russo, G. S. Kanade, H. Kusaba, Y. Teraoka, N. Labhsetwar, Catal. Lett. (2009) 132:248–252, DOI 10.1007/s10562-009-0092-y.

[12] **"Adsorption and reactivity of nitrogen oxides (NO₂, NO, N₂O) on Fe–zeolites"** M. Rivallan, G. Ricchiardi, S. Bordiga, A. Zecchina, Journal of Catalysis 264 (2009) 104-116.

[13] **"The simultaneous catalytic reduction of NO and N₂O by NH₃ using an Fe-zeolite-beta catalyst"** B. Coqa, M. Mauvezin, G. Delahay, J-B. Butet, S. Kieger, Applied Catalysis B: Environmental 27 (2000) 193-198.

[14] **"Catalytic decomposition of N₂O and catalytic reduction of N₂O and N₂O + NO by NH₃ in the presence of O₂ over Fe-zeolite"** A. Guzmán-Vargas, G. Delahay, B. Coq, Applied Catalysis B: Environmental 42 (2006) 369-379.

[15] **"N₂O-mediated propane oxidative dehydrogenation over Fe-zeolites. TEOM studies for

continuous propylene production in a cyclically-operated reactor" J. Perez-Ramirez, A. Gallardo-Llamas, C. Daniel, C. Mirodatos, Chemical Engineering Science 59 (2004) 5535-5543.

[16] "Catalytic decomposition of nitrous oxide over calcined cobalt aluminum hydrotalcites" S. Kannan, C.S. Swamy, Catalysis Today 53 (1999) 725-737.

[17] "Excellent catalytic performance of $Zn_xCo_{1-x}Co_2O_4$ spinel catalysts for the decomposition of nitrous oxide" L. Yan, T. Ren, X. Wang, Q. Gao, D. Ji, J. Suo, Catalysis Communications 24(2003) 505-509.

[18] "N_2O catalytic decomposition over various spinel-type oxides" N. Russo, D. Fino, G. Saracco, V. Specchia, Catalysis Today 119 (2007) 228-232.

[19] "Catalytic decomposition of N_2O over CeO_2 promoted Co_3O_4 spinel catalyst" L. Xue, C. Zhang, H. He, Y. Teraoka, Applied Catalysis B: Environmental 75(2007) 167-174.

[20] "A study on N_2O catalytic decomposition over Co/ MgO catalysts" Q. Shen, L. Li, J. Li, H. Tian, Z. Hao, Journal of Hazardous Materials 163 (2009) 1332-1337.

[21] "Nitrous oxide decomposition over alkali promoted magnesium cobaltite catalysts" B. M. Abu-Zied (2009), Applied Catalysis B: Environmental, Manuscript Draft, Manuscript Number: APCATB-D-09-00973.

[22] "Optimization of Multicomponent Cobalt Spinel Catalyst for N_2O Abatement from Nitric Acid Plant Tail Gases: Laboratory and Pilot Plant Studies" P. Stelmachowski, F. Zasada, G. Maniak, P. Granger, M. Inger, M. Wilk , A. Kotarba, Z. Sojka, Catal. Lett. (2009) 130:637–641, DOI 10.1007/s10562-009-0014-z.

[23] "Effect of Zr^{4+} doping on the stabilization of ZnCo-mixed oxide spinel system and its catalytic activity towards N_2O decomposition" S.N. Basahel, I.H. Abd El-Maksod, B.M. Abu-Zied, M. Mokhtar, Journal of Alloys and Compounds 493 (2009) 630-635.

[24] "Optimized synthesis method for K/Co_3O_4 catalyst towards direct decomposition of N_2O" H. Yoshino, C. H. Ohnishi, S. Hosokawa, K. Wada, M. Inoue , J. Mater. Sci., (2010), DOI 10.1007/s10853-010-4818-4.

[25] "Catalytic decomposition of N_2O over noble and transition metal containing oxides and zeolites. Role of some variables on reactivity". G. Centi, A. Galli, B. Montanari, S. Perathoner, A. Vaccari, Cataysis Today 35 (1997) 113-120.

[26] "Catalytic decomposition of N_2O" J. Haber, T. Machej, J. Janas, M. Nattich Catalysis Today (2004) 15-19.

[27] "Rh–Sr/Al_2O_3 Catalyst for N_2O Decomposition in the Presence of O_2" S. Parres-Esclapez, F. E. Lopez-Suarez, A. Bueno-Lopez, M. J. Illan-Gomez, B. Ura, J. Trawczynski, Top. Catal. (2009) 52:1832–1836, DOI 10.1007/s11244-009-9353-7.

[28] "Decomposition of nitrous oxide by rhodium catalysts: Effect of rhodium particle size and metal oxide support" H. Beyer, J. Emmerich, K. Chatziapostolou, K. Kohler, Applied

Paschalia Taniou, Zoe Ziaka, and Savvas Vasileiadis

Catalysis A: General, Vol.391, Iss.1-2 (2011) 411-416.

[29] **"Mullite-supported Rh catalyst: a promising catalyst for the decomposition of N_2O propellant"** X. Zhao, Y. Cong, F. Lv, L. Li, X. Wang and T. Zhang, The Royal Society of Chemistry, Chem. Commun. 46 (2010) 3028-3030.

[30] "**N_2O-mediated propane oxidative dehydrogenation over Fe-zeolites. TEOM studies for continuous propylene production in a cyclically-operated reactor"** J. Perez-Ramirez, R.A. Gallardo-Llamas, C. Daniel, C. Mirodatos. Chemical Engineering Science 59, (2004) 5535 – 5543.

[31] **"The permeabilities of carbon dioxide, nitrous oxide and oxygen and their mixtures through silicone rubber and cellulose acetate membranes"** R. Hughes and B. Jiang, Gas Sep. Purif. Vol. 9, No. 1. (1995) 27-30.

[32] **"A new membrane tube technique (METT) for continuous gas measurements in soils"** A. Gut, A.Blatter, M.Fahrni, B.E. Lehmann, A. Neftel and Staffelbach, Plant and Soil 198 (1998) 79-88.

[33] **"Permeability functions for pure and mixture gases in silicone rubber and polysulfone membranes: Dependence on pressure and composition"** H. Ettouney, U. Majeed, Journal of Membrane Science 135 (1997) 251-261.

[34] **"Nitrous Oxide High Purification by Membrane Gas Separation"** V. M. Vorotyntsev, P. N. Drozdov, I. V. Vorotyntsev, K. Y. Smirnov, R.Y. Alekseev Nizhny, Inorganic Materials, Vol. 45, No. 11, (2009) 1263–1266, Pleiades Publishing, Ltd.

[35] **"Electro-reduction of nitrogen oxides using steam electrolysis in a proton conducting solid electrolyte membrane reactor (H^+-SEMR)"** K.K. Kalimeri, C.I. Athanasiou, G. E. Marnellos, Solid State Ionics 181 (2009) 223-229.

[36] **"New integrated catalytic membrane processes for enhanced propylene and polypropylene production"**, Z. Ziaka and S. Vasileiadis, Separation Science and Technology Journal, Vol.46, Iss.2, (2011) 224-233.

[37] **"Catalytic decomposition of N_2O over noble and transition metal containing oxides and zeolites. Role of some variables on reactivity".** G. Centi, A. Galli, B. Montanari, S. Perathoner, A. Vaccari, Cataysis Today, 35 (1997) 113-120.

[38] **"Catalytic activity of dispersed CuO phases towards nitrogen oxides (N_2O, NO, and NO_2)"** S. Bennici, A. Gervasini, Applied Catalysis B: Environmental 62 (2006) 336-344.

[39] **"Adsorption of NO and N_2O on Cu-BEA zeolite"** Y. Wang, Z. Lei, R. Zhang, B. Chen, Journal of Molecular Stucture: THEOCHEM 957 (2010) 41-45.

[40] **"Decomposition and reduction of N_2O over copper catalysts"** A. Dandekar, M.A. Vennice, Applied Catalysis B: Environmental 22 (1998) 179-200.

* Corresponding author (Z. Ziaka). Tel/Fax: +30-2310-275473 E-mail addresses: bookeng@hotmail.com, z.ziaka@ihu.edu.gr.

[41] **"In situ characterization of the Ag$^+$ ion-exchanged zeolites and their photocatalytic activity for the decomposition of N$_2$O into N$_2$ and O$_2$ at 298 K"** M. Matsuoka, W-S. Ju, H. Yamashita, M. Anpo, Journal of Photochemistry and Photobiology A: Chemistry 160 (2003) 143-146.

[42] **"An operando optical fiber UV–vis spectroscopic study of the catalytic decomposition of NO and N$_2$O over Cu-ZSM-5"** M. H. Groothaert, K. Lievens, H. Leeman, B. M. Weckhuysen, and R. A. Schoonheydt, Journal of Catalysis 220 (2003) 500-512.

[43] **"Membrane Reactors for Fuel Cells and Environmental Energy Systems**", Z. D. Ziaka and S.P. Vasileiadis, Xlibris Publishing Corporation, Indianapolis, USA, (2009).

[44] **"Membrane reactors for fuel cells and environmental energy systems", Chapter 9,** Z.D. Ziaka and S.P. Vasileiadis, Xlibris Publ., USA (2009).

[45] **"Catalytic Decomposition of N$_2$O"**, Paschalia Taniou, Hellenic Open University Thesis, Patras, (2011).

Dr. Zoe Ziaka is a chemical engineer. She holds a Diploma, a MSc and a PhD in chemical engineering. Her areas of specialization are reaction engineering and reactor design, membrane reactor technology, hydrogen production, fuel cells, environmental engineering, alternative–renewable energy processes, management and applications. She is a member at several European Scientific Administration Committees. She has received several teaching and research awards and has been a faculty member at high ranking Universities in USA and Europe. She has contributed in numerous papers, books, patents and conferences.
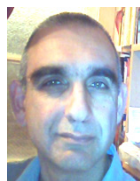
Dr. Savvas Vasileiadis is a chemical and materials engineer. He holds a Diploma, a MSc and a PhD in chemical engineering & materials science. He is a faculty member at the Hellenic Open University. His interests are in catalysis and reaction engineering, fuel cells, membrane reactors and separators, materials engineering and manufacturing. He has commercialized since 1994 methane-steam reforming technology, membrane reactor and fuel cell technology for various fuels including natural gas and renewable feedstocks (such as biogas and biomass feedstocks) through the Zivatech-Engineering, an independent technical enterprise.

Paschalia Taniou is an environmental Engineer, with a diploma from Democritus University of Thrace, Polytechnic Department (Greece). She has experiences in Environmental protection techniques, development of new treatment techniques in air, water and soil protection and experience with wastewater treatment plants, contributed to the deployment, planning and operation of UASB reactors. She has also a MSc degree in Catalysis and Environmental Protection from Hellenic Open University (Greece) with specialization in operation and development of catalytic processes aimed at destroying pollutants and in environmental friendly fuel production. She has obtained a Certificate in Pedagogy and Teaching in 2011, School of Pedagogical and Technological Education, (Greece).